JOURNAL OF GUIDANCE, CONTROL, AND DYNAMICS
Vol. 29, No. 4, July–August 2006

New Global Navigation Satellite System Ambiguity Resolution Method Compared to Existing Approaches

Sandra Verhagen* and Peter J. G. Teunissen†
Delft University of Technology, 2629 HS Delft, The Netherlands

Integer carrier phase ambiguity resolution is the process of resolving unknown cycle ambiguities of double-differenced carrier phase data as integers, and it is a prerequisite for rapid and high-precision global navigation satellite system positioning and navigation. Besides integer estimation, integer ambiguity resolution also involves validation of the integer estimates. In this contribution a new ambiguity resolution method is presented, based on the class of integer aperture estimators, which for the first time reveals an overall approach to the combined problem of integer estimation and validation. Furthermore, it is shown how the different discrimination tests that are currently in use in practice can be cast into the framework of the new approach.

Introduction

THE principle of positioning with a global navigation satellite system (GNSS) is based on determining the distance of at least four GNSS satellites to a receiver. For that purpose two types of distance measurements are employed: the code-based pseudoranges and the carrier-phase measurements. The code observation is based on a binary code, which is modulated on the signal carrier. Using only the code measurements allows positioning with an accuracy of several meters. The phase measurement equals the difference between the phase of the receiver-generated carrier signal at reception time and the phase of the carrier signal generated in the satellite at transmission time. It can be measured to within millimeters. However, an integer number of full cycles is unknown since only the fractional phase can be measured. The distance from receiver to satellite, l, is thus

$$l = \lambda\phi + \lambda N + e \tag{1}$$

with ϕ the phase measurement, λ the wavelength of the carrier signal, N the real-valued ambiguity, and e containing all noise and biases, such as atmospheric delays, multipath, and clock errors. Currently, GPS transmits on two frequencies, with wavelengths of 19.0 and 24.4 cm. In the future a third frequency will be available, with a wavelength of 25.5 cm. The future Galileo system will transmit on four frequencies with wavelengths of 19.0, 23.4, 24.8, and 25.5 cm.

To allow positioning with subcentimeter accuracy, it is thus required to use the very precise carrier-phase measurements, and hence to resolve the unknown integer ambiguities. Furthermore, the principle of differential GNSS is used. Differential GNSS involves the use of linear combinations of the GNSS observations from different satellites and receivers, so that common errors are eliminated or mitigated, such as clock errors and atmospheric delays. Besides the user receiver, one or more reference receivers in known locations are required for that purpose. The GNSS models may differ greatly in complexity and diversity. They range from single-baseline models used for kinematic positioning to multibaseline models used as a tool for studying geodynamic phenomena. The models may or may not have the relative receiver–satellite geometry included. They may also be discriminated as to whether the slave receiver(s) is stationary or in motion, or whether the differential atmospheric delays (ionosphere and troposphere) are included as unknowns. A more detailed description of the GNSS observations and an overview of models can be found in textbooks such as Refs. 1–5.

GNSS ambiguity resolution is the fundamental problem to be addressed in this contribution. Its importance stems from the fact that it is the key to rapid and precise GNSS relative positioning. Once the integer ambiguities are resolved one can take full advantage of the highly precise carrier phase measurements. GNSS ambiguity resolution has important applications in surveying, navigation, geodesy, and geophysics. The applications become more demanding in terms of precision, reliability, availability, and integrity all the time. This is possible thanks to advances in hardware and algorithms. Examples of some highly demanding applications are precision approaches and landing of aircraft,[6,7] attitude determination,[8–11] and formation flying of satellites.[12,13]

To explain the problem of integer ambiguity resolution, we will start with the general GNSS model. Any linear(ized) GNSS relative position model can be cast in the following system of linear observation equations:

$$E\{y\} = Aa + Bb, \qquad a \in \mathbb{Z}^n, \qquad b \in \mathbb{R}^p \tag{2}$$

with $E\{\cdot\}$ the mathematical expectation operator, y the random m-vector of observables, a the n-vector of unknown integer parameters, and b the p-vector of unknown real-valued parameters. The data vector y will then usually consist of the "observed minus computed" single- or multifrequency double-difference phase and/or pseudorange (code) observations accumulated over all observation epochs. The entries of the integer vector a are the double differences of the real-valued carrier phase ambiguities N, expressed in units of cycles. The entries of the real-valued vector b will consist of the remaining unknown parameters, such as baseline components (coordinates) and atmospheric delay parameters (troposphere, ionosphere).

It is the goal of integer ambiguity resolution to exploit the integerness of the ambiguity vector a when estimating the parameters of interest, which are usually the components of b. In the literature on GNSS ambiguity resolution one can recognize two different approaches to this problem, the Bayesian approach and the non-Bayesian approach. In the Bayesian approach, not only the vector of observables y is assumed random, but also the two vectors of unknown parameters, a and b. The improper priors of a and b are then assumed independent and proportional to an integer-centered pulse train and a constant, respectively. The Bayes estimate of b is then taken as the conditional mean of the posterior probability density function (PDF) of b. Examples of Bayesian analyses of GNSS ambiguity resolution can be found in Refs. 14–18. How the Bayesian approach compares to the non-Bayesian approach of integer equivariant minimum variance estimation is shown in Ref. 19.

Received 3 February 2005; revision received 10 October 2005; accepted for publication 12 October 2005.

*Postdoctoral Researcher, Delft Institute of Earth Observation and Space Systems, Kluyverweg 1; A.A.Verhagen@TUDelft.nl.
†Professor, Delft Institute of Earth Observation and Space Systems.

In the present contribution we will use a non-Bayesian approach throughout. Thus only y is considered to be a random vector. The two parameter vectors a and b are unknown and nonrandom. The procedure for solving this GNSS model is then usually divided into three steps. In the first step the integer constraints $a \in \mathbb{Z}^n$ are discarded and a and b are estimated by the method of least squares. As a result, one obtains the so-called "float" solution $\hat{a}$ and $\hat{b}$. This solution is real-valued and it is given as $\hat{a} = (\bar{A}^T Q_y^{-1} \bar{A})^{-1} \bar{A}^T Q_y^{-1} y$ and $\hat{b} = (\bar{B}^T Q_y^{-1} \bar{B})^{-1} \bar{B}^T Q_y^{-1} y$, respectively, with $\bar{A} = P_B^{\perp} A$ and $\bar{B} = P_A^{\perp} B$, where $P_A^{\perp} = I_m - A(A^T Q_y^{-1} A)^{-1} A^T Q_y^{-1}$, $P_B^{\perp} = I_m - B(B^T Q_y^{-1} B)^{-1} B^T Q_y^{-1}$, and Q_y is the variance matrix of y.

Then, in the second step, the float solution $\hat{a}$ is further adjusted to take the integerness of the ambiguities into account. This is done by mapping $\hat{a}$ to an integer vector $\check{a}$,

$$\check{a} = S(\hat{a}) \tag{3}$$

with $S : \mathbb{R}^n \mapsto \mathbb{Z}^n$. This estimator is then used in the final step to adjust the float estimator $\hat{b}$. As a result one obtains the so-called "fixed" estimator of b as

$$\check{b} = \hat{b} - Q_{\hat{b}\hat{a}} Q_{\hat{a}}^{-1} (\hat{a} - \check{a}) \tag{4}$$

in which $Q_{\hat{a}}$ denotes the variance matrix of $\hat{a}$ and $Q_{\hat{b}\hat{a}}$ denotes the covariance matrix of $\hat{b}$ and $\hat{a}$. The matrix product $Q_{\hat{b}\hat{a}} Q_{\hat{a}}^{-1}$, when expressed in A and B, reads $Q_{\hat{b}\hat{a}} Q_{\hat{a}}^{-1} = (\bar{B}^T Q_y^{-1} \bar{B})^{-1} \bar{B}^T Q_y^{-1} \bar{A}$.

The above three-step procedure is still ambiguous in the sense that it leaves room for choosing the n-dimensional map S. Different choices for S will lead to different ambiguity estimators and thus also to different baseline estimators $\check{b}$. Examples of integer estimators that are in use in practice are the ones based on integer rounding, integer bootstrapping, and integer least squares.

Next to the integer estimation step, integer validation also plays a crucial role in the process of ambiguity resolution. After all, even when one uses an optimal, or close to optimal, integer ambiguity estimator, one can still come up with an unacceptable integer solution. Unfortunately, however, there does not yet exist a rigorous probabilistic theory for the validation of integer ambiguities. Various validation procedures have been proposed in the literature. Some seem to have good performance; others, however, can be shown to perform poorly, whereas still others perform poorly in some cases and well in other cases. One of the earliest and most popular ways of validating the integer ambiguity solution is to make use of the so-called ratio test. The test statistic of the ratio test is defined as the ratio of the squared norm of the "best" ambiguity residual vector and the squared norm of the "second-best" ambiguity residual vector. The computed integer ambiguity solution is then rejected in favor of the float solution when this ratio exceeds a certain user-defined threshold. Also, the so-called F-ratio test, the difference test, and the projector test are in use in practice. They also are defined so that the test statistics depend on the best and second-best ambiguity estimators.

In this contribution we will study the properties and underlying concept of these tests. It will be shown that the procedure underlying the tests can be given a firm theoretical footing, but one that differs significantly from the ones described in the literature. For the practical user of the tests this has the important consequence that the tests have to be evaluated differently then thought so far.

The firm theoretical basis that can be given to the tests is made possible by the recently introduced theory of integer aperture (IA) inference.[20] The required ingredients of this theory will be briefly described. It will be shown that the procedure underlying the ratio test, the difference test, and the projector test are all members from the class of integer aperture estimators. This allows us 1) to quantify and qualify the acceptance region of the tests, 2) to give an exact and overall probabilistic evaluation of the combined integer estimation and validation solution, and 3) to show the user how he/she needs to compute the critical value of the discrimination test at hand. But it will also be shown how the optimal integer aperture estimator can be defined, so that the probability of correct integer estimation is maximized, and at the same time the failure rate will not exceed a user-defined threshold.

The outline of this contribution is as follows. First the theory of integer estimation is reviewed. Then the theory of integer aperture estimation is introduced. The following sections are then devoted to the various tests that are currently in use in practice. For each of the tests it will be proven that the underlying procedures are indeed members from the class of integer aperture estimators, and it will be shown how the corresponding acceptance regions are constructed. Finally, the properties of the tests will be evaluated based on simulations. The results will also be used to compare the performance of the discrimination tests with that of the optimal integer aperture estimator.

Integer Ambiguity Resolution

Integer Estimation

We start by introducing the class of integer estimators. Because $S : \mathbb{R}^n \mapsto \mathbb{Z}^n$ in Eq. (3) is a many-to-one map, different real-valued vectors will be mapped by S to the same integer vector. Therefore, a subset $S_z \subset \mathbb{R}^n$ can be assigned to each integer vector $z \in \mathbb{Z}^n$:

$$S_z = \{x \in \mathbb{R}^n \mid z = S(x), z \in \mathbb{Z}^n\} \tag{5}$$

This subset S_z contains all real-valued float ambiguity vectors that will be mapped to the same integer vector z, and it is called the pull-in region of z.[21,22] One can now define the class of integer estimators through the conditions that these pull-in regions have to fulfill. We require the pull-in regions to satisfy the following three conditions:

$$\begin{aligned} &1) \quad \bigcup_{z \in \mathbb{Z}^n} S_z = \mathbb{R}^n \\ &2) \quad \mathrm{Int}(S_u) \bigcap \mathrm{Int}(S_z) = \emptyset, \qquad \forall u, z \in \mathbb{Z}^n, \qquad u \neq z \\ &3) \quad S_z = z + S_0, \qquad \forall z \in \mathbb{Z}^n \end{aligned} \tag{6}$$

where "Int" denotes the interior of the subset. Hence, the pull-in regions are required to be translationally invariant and to cover $\mathbb{R}^n$ without gaps and overlaps. In Ref. 23 the motivation for this definition is given. It follows that every integer estimator $\check{a}$ can now be expressed as

$$\check{a} = \sum_{z \in \mathbb{Z}^n} z s_z(\hat{a}) \tag{7}$$

with the indicator function, $s_z(x)$, defined as

$$s_z(x) = \begin{cases} 1 & \text{if} \quad x \in S_z \\ 0 & \text{otherwise} \end{cases} \tag{8}$$

Examples of estimators that belong to this class of integer estimators are integer rounding, integer bootstrapping, and integer least squares (ILS). Their pull-in regions are the multivariate versions of a square, a parallelogram, and a hexagon, respectively. The pull-in regions always have a volume equal to one.

It will be clear that the outcome of an integer estimator should only be used if one has enough confidence in the solution. Hence, one needs to evaluate the distribution of

$$\check{a} = \sum_{z \in \mathbb{Z}^n} z s_z(\hat{a})$$

This distribution, denoted as $P(\check{a} = z)$, is a probability mass function with zero masses at noninteger points, and nonzero masses at some or all integer points. With the division of $\mathbb{R}^n$ into mutually exclusive pull-in regions, the distribution of $\check{a}$ follows as[24]

$$P(\check{a} = z) = P(\hat{a} \in S_z) = \int_{S_z} f_{\hat{a}}(x)\, \mathrm{d}x, \qquad z \in \mathbb{Z}^n \tag{9}$$

where $f_{\hat{a}}(x)$ is the continuous probability density function (PDF) of the float ambiguity vector $\hat{a}$. In most GNSS applications the data are assumed to be normally distributed, and thus the estimator $\hat{a}$ will

be normally distributed too with mean $a \in \mathbb{Z}^n$ and variance matrix $Q_{\hat{a}}$. The PDF is then given by

$$f_{\hat{a}}(x) = C \exp\left\{-\tfrac{1}{2}\|x-a\|^2_{Q_{\hat{a}}}\right\} \tag{10}$$

where C is a normalization constant.

From the probability mass function of $\check{a}$, one is particularly interested in the probability of correct integer estimation, the so-called success rate of ambiguity resolution. The success rate $P_s = P(\check{a} = a)$ follows from Eq. (9) as

$$P_s = P(\check{a} = a) = \int_{S_a} f_{\hat{a}}(x)\,\mathrm{d}x = \int_{S_0} f_{\hat{a}}(x+a)\,\mathrm{d}x \tag{11}$$

Note that the success rate can be computed without knowledge of a for any distribution of $\hat{a}$ that is translated over a when the mean a is subtracted from the stochastic variable $\hat{a}$, that, $f_{\hat{a}}(x) = f_{\hat{a}-a}(x-a)$. Obviously, this is the case for the normal distribution of Eq. (10).

Since the success rate depends on the pull-in region and therefore on the chosen integer estimator, it is of importance to know which integer estimator maximizes the probability of correct integer estimation. For an arbitrary PDF the solution is given in Ref. 25. For elliptically contoured distributions, such as the multivariate normal distribution, the ILS-estimator can be shown to be the optimal estimator.[23] The ILS estimator is given as

$$\check{a}_{\mathrm{LS}} = \arg\min_{z \in \mathbb{Z}^n} \|\hat{a} - z\|^2_{Q_{\hat{a}}} \tag{12}$$

with the squared norm $\|\cdot\|^2_Q = (\cdot)^T Q^{-1}(\cdot)$. Note, since

$$\|y - Aa - Bb\|^2_{Q_y} = \|y - A\hat{a} - B\hat{b}\|^2_{Q_y} + \|\hat{a} - a\|^2_{Q_{\hat{a}}}$$

$$+ \|\hat{b} - b - Q_{\hat{b}\hat{a}}Q_{\hat{a}}^{-1}(\hat{a}-a)\|^2_{(B^T Q_y^{-1} B)^{-1}}$$

that $\check{a}_{\mathrm{LS}}$ and $\check{b}_{\mathrm{LS}} = \hat{b} - Q_{\hat{b}\hat{a}}Q_{\hat{a}}^{-1}(\hat{a} - \check{a}_{\mathrm{LS}})$ is the solution of $\min_{a\in\mathbb{Z}^n, b\in\mathbb{R}^n} \|y - Aa - Bb\|^2_{Q_y}$ (Ref. 26).

In contrast to integer rounding and integer bootstrapping, an integer search is needed to compute $\check{a}_{\mathrm{LS}}$. The ILS-procedure is mechanized in the LAMBDA (least-squares ambiguity decorrelation adjustment) method,[26–28] which is currently one of the most applied methods for GNSS carrier phase ambiguity resolution. Practical results obtained with it can be found, for example, in Refs. 9, 11, 13, 21, and 29–41. Further studies on the decorrelation step of the LAMBDA method can be found in Refs. 42–46.

To evaluate the success rate of ILS-estimation, we need to integrate the PDF over the ILS pull-in region; cf. Eq. (11). The ILS pull-in region that belongs to the integer vector z is given as

$$S_z = \left\{x \in \mathbb{R}^n \,\middle|\, \|x-z\|^2_{Q_{\hat{a}}} \le \|x-u\|^2_{Q_{\hat{a}}}, \forall u \in \mathbb{Z}^n\right\}$$

$$= \bigcap_{c\in\mathbb{Z}^n} \left\{x \in \mathbb{R}^n \,\middle|\, \left|c^T Q_{\hat{a}}^{-1}(x-z)\right| \le \tfrac{1}{2}\|c\|^2_{Q_{\hat{a}}}\right\} \tag{13}$$

Hence, the ILS pull-in regions are constructed as intersecting half-spaces, which are bounded by the plane orthogonal to $(u-z)$, $u \in \mathbb{Z}^n$, and passing through $\frac{1}{2}(u+z)$. Because of the complexity of the geometry of the ILS pull-in region, it is not possible to give an exact evaluation of the ILS success rate. One has to resort to Monte Carlo methods or to the use of lower and upper bounds. Fortunately sharp bounds are available for evaluating the ILS success rate. An overview and evaluation of lower and upper bounds is given in Ref. 47.

Integer Validation in Practice

It is important to realize that the success rate as introduced here is a diagnostic measure for the expected performance of the integer estimator, but not of its actual performance. Thus even if the success rate is considered large enough, it can still happen that an actual outcome of the integer estimator is erroneous. This is why in practice so-called discrimination tests are used. Of course, one can never be sure whether the integer outcome is correct or not. But what one can do is to single out integer outcomes that are suspect. This is the whole purpose of the discrimination tests. Several such tests have been proposed in the literature and are currently in use in practice.[38,48–55]

All these tests compare in one way or another the ILS solution $\check{a}_{\mathrm{LS}}$ with a so-called "second best" integer solution $\check{a}'$. Based on this comparison, the outcome of the discrimination tests is either to accept the integer solution $\check{a}_{\mathrm{LS}}$, or to reject it in favor of the float solution $\hat{a}$. Examples of discrimination tests are the ratio test, the difference test, and the projector test.

Unfortunately, all discrimination tests proposed in the literature until now lack a sound theoretical basis. They have been introduced in an ad hoc way, their evaluation is based on the incorrect assumption that $\check{a}_{\mathrm{LS}}$ and $\check{a}'$ are nonrandom, they use critical values that are chosen as fixed values, and their performance is treated separately from the performance of the integer estimator. An overview of how these tests are used in practice and their pitfalls is given in Ref. 56. In this contribution it will be shown that it is possible to give a theoretical foundation to these tests. It will be shown that the tests all fit in the framework of the new class of integer aperture estimators. As a result, the probabilistic evaluation of integer aperture estimation makes it possible to give an overall evaluation of both the integer estimation part and the integer discrimination part.

Integer Aperture Estimation

The idea behind IA estimation is to distinguish between the following three situations: *success* if the integer ambiguity is estimated correctly, *failure* if the integer ambiguity is estimated incorrectly, and *undecided* if the real-valued float solution is maintained. These three possible outcomes can be brought together in one estimator if one drops the condition that there may be no gaps between the pull-in regions. To achieve this, we now take, instead of the whole space $\mathbb{R}^n$, a subset $\Omega \subset \mathbb{R}^n$ as the region for which $\hat{a}$ is mapped to an integer. Thus $\hat{a}$ is mapped to an integer if $\hat{a} \in \Omega$ and the float solution is maintained if $\hat{a} \in \mathbb{R}^n \setminus \Omega$. The region Ω is called the aperture space. To ensure that any integer-perturbed version of $\hat{a}$ gets mapped to an integer whenever $\hat{a}$ itself is mapped to an integer, the aperture space is required to be translationally invariant, $\Omega = \Omega + z$, $\forall z \in \mathbb{Z}^n$. To determine to which integer the float solution is mapped, we introduce

$$\Omega_z = \Omega \cap S_z, \qquad \forall z \in \mathbb{Z}^n \tag{14}$$

where S_z is a pull-in region satisfying the conditions of Eq. (6). Then

$$\begin{aligned}
&1) \quad \bigcap_{z\in\mathbb{Z}^n} \Omega_z = \Omega \\
&2) \quad \mathrm{Int}(\Omega_u) \bigcap \mathrm{Int}(\Omega_z) = \emptyset, \qquad \forall u, z \in Z^n, \qquad u \neq z \\
&3) \quad \Omega_z = z + \Omega_0, \qquad \forall z \in Z^n
\end{aligned} \tag{15}$$

This shows that the subsets $\Omega_z \subset S_z$ satisfy conditions similar to those satisfied by S_z, with $\mathbb{R}^n$ replaced by $\Omega \subset \mathbb{R}^n$. The IA estimator can now be defined as follows. The IA estimator maps the float solution $\hat{a}$ to the integer vector z when $\hat{a} \in \Omega_z$ and it maps the float solution to itself when $\hat{a} \notin \Omega$. Any IA estimator, denoted as $\bar{a}$, can then be expressed as

$$\bar{a} = \sum_{z\in\mathbb{Z}^n} z\omega_z(\hat{a}) + \hat{a}\left(1 - \sum_{z\in\mathbb{Z}^n} \omega_z(\hat{a})\right) \tag{16}$$

with the indicator function, $\omega_z(x)$, defined as

$$\omega_z(x) = \begin{cases} 1 & \text{if } x \in \Omega_z \\ 0 & \text{otherwise} \end{cases} \tag{17}$$

Compare Eq. (16) with Eq. (7). Note that an IA estimator is completely defined once Ω_0 is chosen. This subset can be seen as an adjustable pull-in region with two limiting cases: the limiting case in which Ω_0 is empty and the limiting case in which Ω_0 equals S_0. In the first case the IA estimator becomes identical to the float estimator $\hat{a}$, and in the second case the IA estimator becomes identical to an integer estimator. The subset Ω_0 therefore determines the *aperture* of the pull-in region.

To be able to evaluate an IA estimator, we need to distinguish between the following three cases:

$\hat{a} \in \Omega_a$	success: correct integer estimation
$\hat{a} \in \Omega \setminus \{\Omega_a\}$	failure: incorrect integer estimation
$\hat{a} \notin \Omega$	undecided: ambiguity not fixed to an integer

where $\Omega \setminus \Omega_a$ means that Ω_a is deleted from the set Ω, with a being the unknown integer ambiguity vector.

The corresponding probabilities of success (s), failure (f), and undecidedness (u) are given by

$$P_s = P(\bar{a} = a) = \int_{\Omega_a} f_{\hat{a}}(x)\,\mathrm{d}x$$

$$P_f = \sum_{z \in \mathbb{Z}^n \setminus \{a\}} \int_{\Omega_z} f_{\hat{a}}(x)\,\mathrm{d}x = \int_{\Omega_0} f_{\check{\epsilon}}(x)\,\mathrm{d}x - \int_{\Omega_a} f_{\hat{a}}(x)\,\mathrm{d}x$$

$$P_u = 1 - P_s - P_f = 1 - \int_{\Omega_0} f_{\check{\epsilon}}(x)\,\mathrm{d}x \tag{18}$$

The first two probabilities are referred to as success rate and failure rate, respectively. The expression for the failure rate is obtained by using the probability density function of the ambiguity residuals $\check{\epsilon} = \hat{a} - \check{a}$ (Ref. 24):

$$f_{\check{\epsilon}}(x) = \sum_{z \in \mathbb{Z}^n} f_{\hat{a}}(x + z) s_0(x) \tag{19}$$

with $s_0(x)$ the indicator function of Eq. (8), and $\check{\epsilon}$ the estimator of $\epsilon = \hat{a} - a$ with $f_\epsilon(x) = f_{\hat{a}}(x + a)$. Evaluation of the PDF in Eq. (19) involves an infinite sum. In Ref. 57 it is demonstrated how a finite integer set can be chosen for which this sum converges with an approximation error on the order of 10^{-8} within reasonable computation times.

As mentioned earlier, for a user it is especially important that the failure rate be below a certain limit. The approach of integer aperture estimation now allows us to choose a threshold for the failure rate, and then determine the *size* of the aperture pull-in regions such that the failure rate will be equal to or below this threshold. Once the failure rate P_f has been chosen, the various other probabilities can be computed. For a user, knowledge of the unconditional success rate $P_s = P(\bar{a} = a)$ and the conditional success rate $P(\bar{a} = a | \hat{a} \in \Omega)$ is particularly important. The unconditional success rate describes the probability of a correct outcome, whereas the conditional success rate describes the probability that an integer outcome is correct. Because $P_s + P_f$ equals the probability of an integer outcome, the conditional success rate is given by the ratio $P_s/(P_s + P_f)$. Hence, the conditional success rate will be close to one when the failure rate is chosen close to zero. This implies that one can have very high confidence in the correctness of the integer outcomes of the integer aperture estimator, even for modest values of the unconditional success rate. IR one used an integer estimator instead of an integer aperture estimator, then such a high confidence could only be reached once the success rate of the integer estimator was close to one; cf. Eq. (11).

Application of this fixed failure rate approach means that implicitly the ambiguity estimate is validated using a sound criterion. This is an important result, because it means that the integer aperture estimation method for the first time reveals an overall approach to the problem of integer ambiguity estimation and validation, which allows probabilistic evaluation of the final solution.

Perhaps superfluously, we note that these properties hold true on the average, but not necessarily for the individual outcomes of a single experiment. This is inherent in any probabilistic evaluation of random phenomena. Thus an outcome $\bar{a} = \hat{a}$, for instance, is no guarantee that the corresponding rejected outcome $\check{a}$ is further apart from the correct integer a than $\hat{a}$ is from a. The probability, however, that the estimator $\bar{a}$ is further apart from a than the estimator $\hat{a}$ is from a is less than the failure rate and therefore small.

So far, we have not specified the aperture pull-in regions completely. There are still several options left with respect to the choice of the *shape* of the aperture pull-in regions. In the following sections it will be shown that the procedures underlying the discrimination tests are all examples of integer aperture estimators. For the different tests it will be shown how the shape of the aperture pull-in regions is determined.

Optimal Integer Aperture Estimation

It is also possible to define an *optimal* integer aperture estimator by requiring that the success rate will be maximized for a given failure rate; that is, the optimization problem is given by

$$\max_{\Omega_0 = \Omega \cap S_0} P_s \quad \text{subject to} \quad P_f = \beta \tag{20}$$

where β is the chosen value for the fixed failure rate. For an arbitrary PDF of $\hat{a}$ the solution to the optimization problem is presented in Ref. 58. For elliptically contoured distributions, the optimal integer aperture estimator can be regarded as a combination of ILS-estimation and the following test:

$$\text{Accept } \check{a}_{\mathrm{LS}} \text{ iff:} \quad \frac{f_{\check{\epsilon}}(\check{\epsilon}_{\mathrm{LS}})}{f_{\epsilon}(\check{\epsilon}_{\mathrm{LS}})} \leq \mu, \qquad \mu > 1 \tag{21}$$

with $\check{\epsilon}_{\mathrm{LS}} = \hat{a} - \check{a}_{\mathrm{LS}}$. Note that for the computation of $f_\epsilon(\check{\epsilon}_{\mathrm{LS}})$ and $f_{\check{\epsilon}}(\check{\epsilon}_{\mathrm{LS}})$ knowledge of a is not needed for any distribution for which $f_{\hat{a}}(x) = f_{\hat{a}-a}(x - a)$. If for instance the normal distribution is used, $f_\epsilon(\check{\epsilon}_{\mathrm{LS}}) = f_{\hat{a}}(\check{\epsilon}_{\mathrm{LS}} + a)$ can be computed with Eq. (10), and then a is eliminated. Equation (19) is used for the computation of $f_{\check{\epsilon}}(\check{\epsilon}_{\mathrm{LS}})$. Because of the infinite sum over all integers, again knowledge of the true integer a is not required. Furthermore note that, because $\check{\epsilon}_{\mathrm{LS}} \in S_0$, the factor $s_0(\check{\epsilon}_{\mathrm{LS}})$, which is needed for the evaluation of $f_{\check{\epsilon}}(\check{\epsilon}_{\mathrm{LS}})$ with Eq. (19), will always come out to be 1. Hence, with the normal distribution for the float ambiguity estimator, the ratio in Eq. (21) becomes

$$\frac{f_{\check{\epsilon}}(\check{\epsilon}_{\mathrm{LS}})}{f_{\epsilon}(\check{\epsilon}_{\mathrm{LS}})} = \frac{\sum_{z \in \mathbb{Z}^n} \exp\left\{-\frac{1}{2}\|\check{\epsilon}_{\mathrm{LS}} + z\|^2_{Q_{\hat{a}}}\right\}}{\exp\left\{-\frac{1}{2}\|\check{\epsilon}_{\mathrm{LS}}\|^2_{Q_{\hat{a}}}\right\}}$$

We note that the above optimal integer aperture estimator can also be interpreted from two different alternative viewpoints. The first one is a Bayesian viewpoint in which all parameters are considered random, with a diffuse prior assumption for the integer parameters. In this context, the ratio on the left-hand side of the inequality in Eq. (21) is equal to the reciprocal marginal a posteriori probability of $\check{a}_{\mathrm{LS}}$ being the true integer vector.[15,16] The second alternative viewpoint is provided by the non-Bayesian penalized ambiguity estimator introduced in Ref. 59. With this estimator the user is given the possibility of assigning penalties to each of the possible outcomes of the estimator. The average of all penalties is minimized by the penalized ambiguity estimator. When penalties are assigned to the three cases, success, failure, and undecided, the structure of the penalized ambiguity estimator is the same as that of the optimal integer aperture estimator. The parameter μ of Eq. (21) will then be a function of the assigned penalties.

The optimal test of Eq. (21) has the highest possible success rate, unconditional as well as conditional, for a given failure rate. The critical value μ is referred to as the aperture parameter, because it determines the size of the aperture pull-in regions; it is completely determined by the constraint on the failure rate, $P_f = \beta$. The higher the failure rate, the higher the value of μ, and hence the larger the aperture of Ω_0. The aperture parameter μ cannot be smaller than one, because the numerator of Eq. (21) is always larger than the denominator. If the failure rate is required to be smaller than the success rate, which is a reasonable condition, it can be shown that μ must then be smaller than 2, because $P_f \leq (\mu - 1) P_s$ (Ref. 58).

The computational steps involved in computing the optimal integer aperture estimator are now as follows. First compute the integer least-squares solution, $\check{a}_{\mathrm{LS}}$. Then form the ambiguity residual, $\check{\epsilon}_{\mathrm{LS}} = \hat{a} - \check{a}_{\mathrm{LS}}$, and check whether $\check{\epsilon}_{\mathrm{LS}} \in \Omega_0$; cf. the test of Eq. (21). If

this is the case then the outcome of the optimal estimator is $\check{a}_{\mathrm{LS}}$, otherwise the outcome is $\hat{a}$. For computational efficiency it is advisable to compute $\check{a}_{\mathrm{LS}}$ with the LAMBDA method and use the LAMBDA-transformed ambiguities also for the evaluation of $\check{\epsilon}_{\mathrm{LS}} \in \Omega_0$.

In the next and following sections we will consider four discrimination tests that are currently in use and show that each of the underlying procedures is an example of an IA-estimator. The tests considered are the ratio test, the F-ratio test, the difference test, and the projector test.

Ratio Test

A very popular discrimination test is the one introduced in Ref. 50. It is given by

$$\text{Accept } \check{a}_{\mathrm{LS}} \text{ iff:} \quad \frac{\|\hat{a}-\check{a}_2\|^2_{Q_{\hat{a}}}}{\|\hat{a}-\check{a}_{\mathrm{LS}}\|^2_{Q_{\hat{a}}}} = \frac{R_2}{R_1} \geq c \tag{22}$$

where the notation R_i is used for the squared norm of ambiguity residuals of the best ($i=1$) and second-best ($i=2$) integer solution, $\check{a}_{\mathrm{LS}}$ and $\check{a}_2$ respectively, as measured by the squared norm of the ambiguity residual vector.

A problem with this approach is that the determination of the critical value is not straightforward. In Ref. 50 the test statistic is derived by applying the classical theory of hypothesis testing. However, to determine the critical value, incorrect assumptions are made on the probability distributions of the parameters involved. Other approaches have also been proposed in the literature, all based on choosing a fixed critical value for test (22), without a theoretical basis. See Ref. 60 for more detailed comments on the approaches proposed in the literature.

Another point of criticism of the ratio test is that the combined integer estimation and validation solution lacks an overall probabilistic evaluation.

But, despite this criticism, integer validation based on the ratio test is often reported to work satisfactorily in practice.

Integer Aperture Estimation with the Ratio Test

It will be shown that the procedure underlying the ratio test is a member of the class of integer aperture estimators. In the sequel the inverse of the test statistic of Eq. (22) will be used:

$$\text{Accept } \check{a}_{\mathrm{LS}} \text{ iff:} \quad R_1/R_2 \leq \mu, \qquad 0<\mu\leq 1 \tag{23}$$

The critical value is denoted as μ. For the following to be true, the condition $0<\mu\leq 1$ must be fulfilled. The acceptance region or aperture space is then given as

$$\Omega = \left\{x\in\mathbb{R}^n \mid \|x-\check{x}_{\mathrm{LS}}\|^2_{Q_{\hat{a}}} \leq \mu\|x-\check{x}_2\|^2_{Q_{\hat{a}}}, 0<\mu\leq 1\right\} \tag{24}$$

with $\check{x}_{\mathrm{LS}}$ and $\check{x}_2$ the best and second-best estimators of x, respectively. Let $\Omega_z = \Omega \cap S_z$; that is, Ω_z is the intersection of Ω with the ILS pull-in region as defined in Eq. (13). Then all conditions of Eq. (15) are fulfilled, because

$$\begin{cases} \Omega_0 = \left\{x\in\mathbb{R}^n \mid \|x\|^2_{Q_{\hat{a}}} \leq \mu\|x-z\|^2_{Q_{\hat{a}}}, \forall z\in\mathbb{Z}^n\setminus\{0\}\right\} \\ \Omega_z = \Omega_0 + z, \qquad \forall z\in\mathbb{Z}^n \\ \Omega = \bigcup\limits_{z\in\mathbb{Z}^n} \Omega_z \end{cases} \tag{25}$$

The proof is as follows:

$$\begin{aligned}
\Omega_z &= \Omega\cap S_z \\
&= \left\{x\in S_z \mid \|x-\check{x}_{\mathrm{LS}}\|^2_{Q_{\hat{a}}} \leq \mu\|x-\check{x}_2\|^2_{Q_{\hat{a}}}, 0<\mu\leq 1\right\} \\
&= \left\{x\in S_z \mid \|x-\check{x}_{\mathrm{LS}}\|^2_{Q_{\hat{a}}} \leq \mu\|x-u\|^2_{Q_{\hat{a}}}, \forall u\in\mathbb{Z}^n\setminus\{\check{x}_{\mathrm{LS}}\}, \right. \\
&\qquad \left. 0<\mu\leq 1\right\} \\
&= \left\{x\in S_z \mid \|x-z\|^2_{Q_{\hat{a}}} \leq \mu\|x-u\|^2_{Q_{\hat{a}}}, \forall u\in\mathbb{Z}^n\setminus\{z\}, 0<\mu\leq 1\right\} \\
&= \left\{x\in\mathbb{R}^n \mid \|x-z\|^2_{Q_{\hat{a}}} \leq \mu\|x-u\|^2_{Q_{\hat{a}}}, \forall u\in\mathbb{Z}^n\setminus\{z\}, \right. \\
&\qquad \left. 0<\mu\leq 1\right\} \\
&= \left\{x\in\mathbb{R}^n \mid \|y\|^2_{Q_{\hat{a}}} \leq \mu\|y-v\|^2_{Q_{\hat{a}}}, \forall v\in\mathbb{Z}^n\setminus\{0\}, \right. \\
&\qquad \left. x=y+z, 0<\mu\leq 1\right\} \\
&= \Omega\cap S_0 + z \\
&= \Omega_0 + z
\end{aligned}$$

The first two equalities follow from the definition of the ratio test, and the third from $\|\hat{x}-\check{x}_{\mathrm{LS}}\|^2_{Q_{\hat{a}}} \leq \|\hat{x}-\check{x}_2\|^2_{Q_{\hat{a}}} \leq \|\hat{x}-u\|^2_{Q_{\hat{a}}}$, $\forall u\in\mathbb{Z}^n\setminus\{\check{x}_{\mathrm{LS}}\}$. The fourth equality follows because $\check{x}_{\mathrm{LS}}=z$ is equivalent to $x\in S_z$. The fifth equality follows from the fact that $0<\mu\leq 1$. The last equalities follow from a change of variables, and the definition $\Omega_0=\Omega\cap S_0$. Finally, note that

$$\bigcup_{z\in\mathbb{Z}^n}\Omega_z = \bigcup_{z\in\mathbb{Z}^n}(\Omega\cap S_z) = \Omega\cap\left(\bigcup_{z\in\mathbb{Z}^n} S_z\right)$$

This ends the proof of Eq. (25).

The acceptance region of the ratio test consists thus of an infinite number of regions, each one of which is an integer-translated copy of $\Omega_0\subset S_0$. The acceptance region plays the role of the aperture space, and μ plays the role of the aperture parameter, because it controls the size of the aperture pull-in regions.

It has now been shown that indeed there is a theoretical basis for the ratio test, because the underlying procedure is an integer aperture estimator and there is a sound criterion available for choosing the critical value, or aperture parameter, by means of the fixed-failure-rate approach described at the end of the section on integer aperture estimation.

Ratio Test Aperture Pull-in Region

To understand how the size and shape of the ratio test aperture pull-in region is governed by the aperture parameter and the variance matrix of the float solution, we will now reveal its geometry. From the definition of the aperture pull-in region, Ω_0, the following can be derived:

$$\begin{aligned}
\Omega_0 : \|x\|^2_{Q_{\hat{a}}} &\leq \mu\|x-z\|^2_{Q_{\hat{a}}}, \quad \forall z\in\mathbb{Z}^n\setminus\{0\}, \quad 0<\mu\leq 1 \\
&\Longleftrightarrow \|[(1-\mu)/\mu]x+z\|^2_{Q_{\hat{a}}} \leq (1/\mu)\|z\|^2_{Q_{\hat{a}}}, \quad \forall z\in\mathbb{Z}^n\setminus\{0\} \\
&\Longleftrightarrow \|x+[\mu/(1-\mu)]z\|^2_{Q_{\hat{a}}} \leq [\mu/(1-\mu)^2]\|z\|^2_{Q_{\hat{a}}} \\
&\qquad\qquad \forall z\in\mathbb{Z}^n\setminus\{0\}
\end{aligned} \tag{26}$$

This shows that the aperture pull-in region is equal to the intersection of all ellipsoids with centers $-[\mu/(1-\mu)]z$ and radius $[\sqrt{\mu}/(1-\mu)]\|z\|_{Q_{\hat{a}}}$.

In fact, the intersection region is only determined by the adjacent integers, because $\forall u\in\mathbb{Z}^n$ not being adjacent, Eq. (26) is always fulfilled $\forall x\in S_0$. It follows from Eqs. (24) and (25) that for all $x\in S_0$ on the boundary of Ω_0,

$$\|x\|^2_{Q_{\hat{a}}} = \mu\|x-z\|^2_{Q_{\hat{a}}}, \qquad z = \arg\min_{z\in\mathbb{Z}^n\setminus\{0\}} \|x-z\|^2_{Q_{\hat{a}}}$$

So z is the second closest integer and must therefore be adjacent. Hence, the following is always true:

$$\|x\|^2_{Q_{\hat{a}}} = \mu\|x-z\|^2_{Q_{\hat{a}}} \leq \mu\|x-u\|^2_{Q_{\hat{a}}}, \qquad \forall u\in\mathbb{Z}^n\setminus\{0,z\}$$

and thus the integers u do not have any influence on the boundary of the aperture pull-in region.

This means that the integer least-squares pull-in region S_0 can be split up into sectors, all having another integer z_2 as second closest; that is, $\|x\|^2_{Q_{\hat{a}}} \leq \|x-z_2\|^2_{Q_{\hat{a}}} \leq \|x-u\|^2_{Q_{\hat{a}}}$, $\forall u\in\mathbb{Z}^n\setminus\{0\}$. Within a sector, the aperture pull-in region is then equal to the intersection of the sector with the ellipsoid with center $-[\mu/(1-\mu)]z_2$ and radius

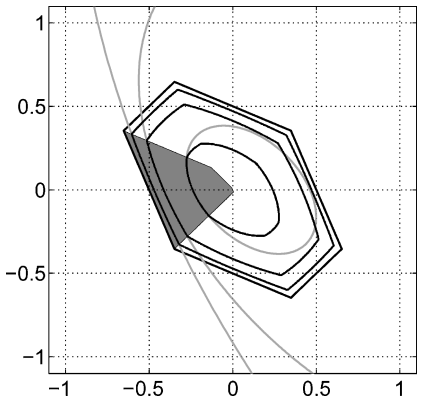

Fig. 1 Geometry of ratio test aperture pull-in region. For all x that fall into the gray region, the second closest integer is $z_2 = [-1\ 0]^T$. The boundary of the aperture pull-in region within this gray region is then equal to the ellipsoid with center $-[\mu/(1-\mu)]z_2$ and radius $[\sqrt{\mu}/(1-\mu)]\|z_2\|_{Q_{\hat{a}}}$. Examples are shown for μ, 0.1, 0.5, and 0.8, respectively. Ellipsoids are gray; aperture pull-in regions black.

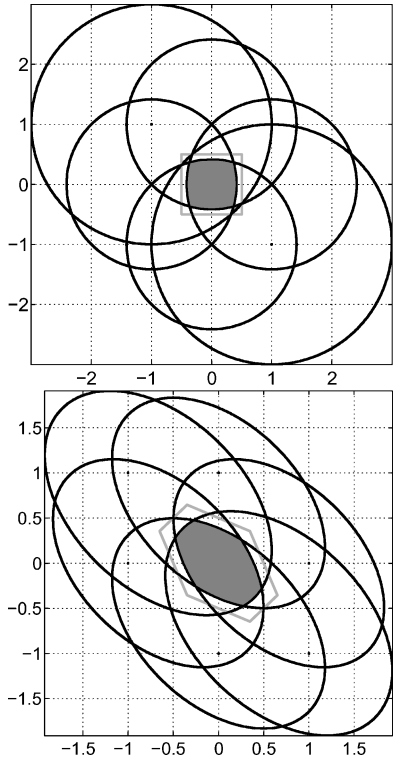

Fig. 2 Geometry of ratio test aperture pull-in region (gray); examples for two variance matrices. Top: identity matrix, $\mu = 0.5$; bottom: Q_1, $\mu = 0.4$.

$[\sqrt{\mu}/(1-\mu)]\|z_2\|_{Q_{\hat{a}}}$. This is illustrated for the two-dimensional case in Fig. 1, with

$$Q_{\hat{a}} = \begin{bmatrix} 0.0865 & -0.0364 \\ -0.0364 & 0.0847 \end{bmatrix} = Q_1 \tag{27}$$

It can be seen that especially for larger μ, the shape of the aperture pull-in region starts to resemble that of the ILS pull-in region. The reason is that for larger μ the radius of the ellipsoid increases, and the center of the ellipsoid is further away, but in the direction of $[z_2, -z_2]$, and the ellipsoid has the same orientation as the ILS pull-in region.

Figure 2 shows two two-dimensional examples of the geometry of the aperture pull-in regions. For a diagonal matrix, the ILS pull-in region becomes square and there are only four adjacent integers. It can be seen in the left panel that indeed only these four integers determine the shape of the aperture pull-in region. With the covariance matrix Q_1 there are six adjacent integers determining the shape.

F-Ratio Test

The F-ratio test also considers the residuals of the best and second-best integer solution, but additionally takes into account the residuals of the complete float solution, $\hat{e} = y - A\hat{a} - B\hat{b}$. It is defined as follows:

$$\text{Accept } \breve{a}_{\text{LS}} \text{ iff: } \quad \frac{\|\hat{e}\|^2_{Q_y} + \|\hat{a} - \breve{a}_2\|^2_{Q_{\hat{a}}}}{\|\hat{e}\|^2_{Q_y} + \|\hat{a} - \breve{a}_{\text{LS}}\|^2_{Q_{\hat{a}}}} \geq c \tag{28}$$

in which $c > 1$ is the chosen critical value. Note that the choice of the critical value is not trivial. In practice, it is often assumed that the test statistic has an F-distribution, so that the critical value can be based on a choice of the level of significance. However, this is not correct because the terms in the numerator and denominator are not independent and not χ^2 distributed.[61] Still, the test in Eq. (28) is often used and seems to work satisfactorily; see, for examples, Refs. 48 and 51. In Ref. 54 it is proposed to use the test statistic with a critical value of $c = 2$.

Integer Aperture Estimation with the *F*-Ratio Test

With the ratio test, the solution is always accepted or rejected for a certain value of the ambiguity residuals and for a certain μ. With the F-ratio test in Eq. (28), however, this is not the case. The test statistic namely depends on the residuals of the complete float solution and on the ambiguity residuals. Using the inverse ratio of Eq. (28), the test becomes

$$\text{Accept } \breve{a}_{\text{LS}} \text{ iff: } \quad \frac{\|\hat{e}\|^2_{Q_y} + \|\hat{a} - \breve{a}_{\text{LS}}\|^2_{Q_{\hat{a}}}}{\|\hat{e}\|^2_{Q_y} + \|\hat{a} - \breve{a}_2\|^2_{Q_{\hat{a}}}} \leq \mu, \qquad 0 < \mu \leq 1 \tag{29}$$

It can be shown that the procedure underlying this test is a member of the class of IA estimators. An integer perturbation of the observations $y + Az$, with $z \in \mathbb{Z}^n$, does not propagate into the least-squares residuals, and $\hat{a}$, $\breve{a}_{\text{LS}}$, and $\breve{a}_2$ all undergo the same change, so that both $\hat{a} - \breve{a}_{\text{LS}}$ and $\hat{a} - \breve{a}_2$ are invariant under the integer perturbation.

F-Ratio Test Aperture Pull-in Region

Similarly to the ratio test, it can be shown what the geometry of the aperture pull-in regions of the F-ratio test IA estimator is:

$$\begin{aligned} \Omega_0 : \|x\|^2_{Q_{\hat{a}}} + \|\hat{e}\|^2_{Q_y} &\leq \mu\left(\|x - z\|^2_{Q_{\hat{a}}} + \|\hat{e}\|^2_{Q_y}\right) \\ &\qquad \forall z \in \mathbb{Z}^n \setminus \{0\}, \qquad 0 < \mu \leq 1 \\ \Longleftrightarrow \|x\|^2_{Q_{\hat{a}}} &\leq \mu\|x - z\|^2_{Q_{\hat{a}}} + (\mu - 1)\|\hat{e}\|^2_{Q_y} \\ \Longleftrightarrow \|x + [\mu/(1-\mu)z]\|^2_{Q_{\hat{a}}} &\leq [\mu/(1-\mu)^2]\|z\|^2_{Q_{\hat{a}}} - \|\hat{e}\|^2_{Q_y} \\ &\qquad \forall z \in \mathbb{Z}^n \setminus \{0\} \end{aligned} \tag{30}$$

So Ω_0 is equal to the intersection of all ellipsoids with centers $-[\mu/(1-\mu)]z$ and radius equal to the square root of the term on the right-hand side of the last inequality in Eq. (30). The shape of the aperture pull-in region is identical to that of the ratio test IA estimator. Obviously, the difference with the ratio test IA estimator is that the radii depend on the sample value of $\hat{e}$. For the same value of μ they will be smaller than or equal to the radii of the ellipsoids determining the ratio test IA aperture pull-in region.

Difference Test

The ratio test statistic is defined as the ratio of the quadratic forms R_1 and R_2. Another approach would be to look at the difference[38] such that the test becomes

$$\text{Accept } \breve{a}_{\text{LS}} \text{ iff: } \quad R_2 - R_1 \geq c \tag{31}$$

It will be clear that again the problem with this test is the choice of the critical value c: only an empirically determined value can be used. Note that in contrast to the ratio test (22), with this test the critical value depends on the variance factor of unit weight, σ^2, if $Q_{\hat{a}} = \sigma^2 G_{\hat{a}}$.

Integer Aperture Estimation with the Difference Test

Similarly to the ratio test, it can be shown that the procedure underlying the difference test (31) belongs to the class of IA estimators. The acceptance region of this test is given as follows:

$$\Omega = \left\{ x \in \mathbb{R}^n \mid \|x - \check{x}_{\mathrm{LS}}\|^2_{Q_{\hat{a}}} \leq \|x - \check{x}_2\|^2_{Q_{\hat{a}}} - \mu \right\} \tag{32}$$

Let $\Omega_z = \Omega \cap S_z$. Then

$$\begin{cases} \Omega_0 = \left\{ x \in \mathbb{R}^n \mid \|x\|^2_{Q_{\hat{a}}} \leq \|x - z\|^2_{Q_{\hat{a}}} - \mu, \forall z \in \mathbb{Z}^n \setminus \{0\} \right\} \\ \Omega_z = \Omega_0 + z, \qquad \forall z \in \mathbb{Z}^n \\ \Omega = \bigcup_{z \in \mathbb{Z}^n} \Omega_z \end{cases} \tag{33}$$

The proof is as follows:

$$\begin{aligned} \Omega_z &= \Omega \cap S_z \\ &= \left\{ x \in S_z \mid \|x - \check{x}_{\mathrm{LS}}\|^2_{Q_{\hat{a}}} \leq \|x - \check{x}_2\|^2_{Q_{\hat{a}}} - \mu \right\} \\ &= \left\{ x \in S_z \mid \|x - \check{x}_{\mathrm{LS}}\|^2_{Q_{\hat{a}}} \leq \|x - u\|^2_{Q_{\hat{a}}} - \mu, \forall u \in \mathbb{Z}^n \setminus \{\check{x}_{\mathrm{LS}}\} \right\} \\ &= \left\{ x \in S_z \mid \|x - z\|^2_{Q_{\hat{a}}} \leq \|x - u\|^2_{Q_{\hat{a}}} - \mu, \forall u \in \mathbb{Z}^n \setminus \{z\} \right\} \\ &= \left\{ x \in \mathbb{R}^n \mid \|x - z\|^2_{Q_{\hat{a}}} \leq \|x - u\|^2_{Q_{\hat{a}}} - \mu, \forall u \in \mathbb{Z}^n \setminus \{z\} \right\} \\ &= \left\{ x \in \mathbb{R}^n \mid \|y\|^2_{Q_{\hat{a}}} \leq \|y - v\|^2_{Q_{\hat{a}}} - \mu, \forall v \in \mathbb{Z}^n \setminus \{0\}, x = y + z \right\} \\ &= \Omega \cap S_0 + z \\ &= \Omega_0 + z \end{aligned}$$

The first two equalities follow from the definition of the difference test, and the third from $\|\hat{x} - \check{x}_{\mathrm{LS}}\|^2_{Q_{\hat{a}}} \leq \|\hat{x} - \check{x}_2\|^2_{Q_{\hat{a}}} \leq \|\hat{x} - u\|^2_{Q_{\hat{a}}}$, $\forall u \in \mathbb{Z}^n \setminus \{\check{x}_{\mathrm{LS}}\}$. The fourth equality follows since $\check{x}_{\mathrm{LS}} = z$ is equivalent to $x \in S_z$. The fifth equality follows from the fact that $\mu \geq 0$. The last equalities follow from a change of variables and the definition of $\Omega_0 = \Omega \cap S_0$. Finally, note that

$$\bigcup_{z \in \mathbb{Z}^n} \Omega_z = \bigcup_{z \in \mathbb{Z}^n} (\Omega \cap S_z) = \Omega \cap \left(\bigcup_{z \in \mathbb{Z}^n} S_z \right)$$

This ends the proof of Eq. (33).

It has been shown that the acceptance region of the difference test consists of an infinite number of integer-translated copies of a subset of the ILS pull-in region S_0. And thus, the difference test procedure is an IA estimator with aperture parameter μ.

Difference Test Aperture Pull-in Region

In a way similar to that of the ratio test aperture pull-in region, the geometry of the aperture pull-in region of the difference test can be revealed. From the definition of Ω_0 it follows that

$$\begin{aligned} &\Omega_0 : \|x\|^2_{Q_{\hat{a}}} \leq \|x - z\|^2_{Q_{\hat{a}}} - \mu, \qquad \forall z \in \mathbb{Z}^n \setminus \{0\}, \qquad \mu \geq 0 \\ &\iff x^T Q_{\hat{a}}^{-1} z \leq \frac{1}{2}\left(\|z\|^2_{Q_{\hat{a}}} - \mu \right) \\ &\iff \frac{z^T Q_{\hat{a}}^{-1} x}{\|z\|_{Q_{\hat{a}}}} \leq \frac{\|z\|^2_{Q_{\hat{a}}} - \mu}{2\|z\|_{Q_{\hat{a}}}} \end{aligned} \tag{34}$$

On the left-hand side of Eq. (34) we recognize the orthogonal projection of x onto the direction z. This shows that the aperture pull-in region Ω_0 is determined by intersecting half-spaces that are bounded by planes orthogonal to z and passing through the points $\frac{1}{2}[1 - (\mu/\|z\|^2_{Q_{\hat{a}}})]z$.

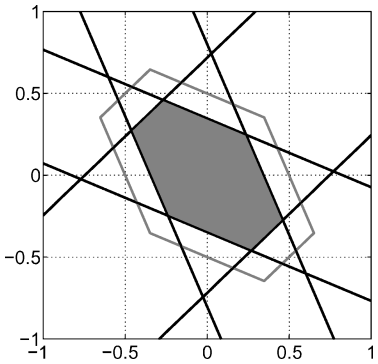

Fig. 3 Geometry of difference test aperture pull-in region (gray) for Q_1, $\mu = 0.4$.

The geometry of Ω_0 is thus very similar to that of the ILS pull-in region S_0, which is also determined by half-spaces bounded by the planes orthogonal to z; see Eq. (13). The difference is that these planes pass through the midpoint $\frac{1}{2}z$, whereas in the case of the difference test this point depends on the distance $\|z\|^2_{Q_{\hat{a}}}$ and on μ. This implies that the difference test aperture pull-in region is a downscaled version of the ILS pull-in region, but that the scaling depends on the direction.

Figure 3 shows a two-dimensional example of the geometry of the aperture pull-in region. The black lines are the planes orthogonal to z and passing through the point $\frac{1}{2}[1 - (\mu/\|z\|^2_{Q_{\hat{a}}})]z$.

Projector Test

The projector test is defined as[52,55]

$$\text{Accept } \check{a}_{\mathrm{LS}} \text{ iff: } \quad \left| \frac{(\check{a}_2 - \check{a}_{\mathrm{LS}})^T Q_{\hat{a}}^{-1} (\hat{a} - \check{a}_{\mathrm{LS}})}{\|\check{a}_2 - \check{a}_{\mathrm{LS}}\|_{Q_{\hat{a}}}} \right| \leq \mu \tag{35}$$

This test is based on the erroneous assumption that the classical theory of hypothesis testing in linear models is applicable to the current situation. The test is referred to as the projector test because the term on the left-hand side of Eq. (35) equals a projector. It projects $\hat{a} - \check{a}_{\mathrm{LS}}$ orthogonally on the direction of $\check{a}_2 - \check{a}_{\mathrm{LS}}$, in the metric of $Q_{\hat{a}}$. Furthermore, note that the following is true:

$$\left| \frac{(\check{a}_2 - \check{a}_{\mathrm{LS}})^T Q_{\hat{a}}^{-1} (\hat{a} - \check{a}_{\mathrm{LS}})}{\|\check{a}_2 - \check{a}_{\mathrm{LS}}\|_{Q_{\hat{a}}}} \right| \leq \frac{1}{2} \|\check{a}_2 - \check{a}_{\mathrm{LS}}\|_{Q_{\hat{a}}} \tag{36}$$

This inequality implies that the fixed solution will always be accepted if $\mu \geq \frac{1}{2}\|\check{a}_2 - \check{a}_{\mathrm{LS}}\|_{Q_{\hat{a}}}$.

Integer Aperture Estimation with the Projector Test

The acceptance region of the projector test is given as

$$\Omega = \left\{ x \in \mathbb{R}^n \mid (\check{x}_{\mathrm{LS}} - \check{x}_2)^T Q_{\hat{a}}^{-1} (x - \check{x}_{\mathrm{LS}}) \leq \mu \|\check{x}_{\mathrm{LS}} - \check{x}_2\|_{Q_{\hat{a}}} \right\} \tag{37}$$

In a way similar to that for the difference test it can be proven that

$$\begin{cases} \Omega_0 = \left\{ x \in S_0 \mid c^T Q_{\hat{a}}^{-1} x \leq \mu \|c\|_{Q_{\hat{a}}}, \quad c = \arg \min_{z \in \mathbb{Z}^n \setminus \{0\}} \|x - z\|^2_{Q_{\hat{a}}} \right\} \\ \Omega_z = \Omega_0 + z, \qquad \forall z \in \mathbb{Z}^n \\ \Omega = \bigcup_{z \in \mathbb{Z}^n} \Omega_z \end{cases} \tag{38}$$

And thus the procedure underlying the projector test also belongs to the class of IA estimators.

Projector Test Aperture Pull-in Region

From Eq. (38) it follows that Ω_0 is bounded by the planes orthogonal to c and passing through μc, and these planes themselves are bounded by the condition that $c = \arg \min_{z \in \mathbb{Z}^n \setminus \{0\}} \|x - z\|^2_{Q_{\hat{a}}}$ for all x on the plane.

Figure 4 shows a two-dimensional example of the geometry of the aperture pull-in region Ω_0. The black lines are the planes orthogonal

to c and passing through μc. For the geometry of Ω_0, these planes are bounded by the condition that $c = \arg\min_{z \in \mathbb{Z}^n \setminus \{0\}} \|x - z\|^2_{Q_{\hat{a}}}$ for all $x \in \Omega_0$. Therefore, sectors within the ILS pull-in region are also shown as alternating gray and white regions, with the sectors containing all x with a certain integer c as second closest integer. The region Ω_0 follows as the region bounded by the intersection of the black lines and the sectors, and by the boundaries of the sectors. This results in a strange nonconvex shape of the aperture pull-in regions in the direction of the vertices of the ILS pull-in region.

Evaluation of the Tests

To illustrate the principle and the properties of the discrimination tests and the optimal test, examples will be given here. These examples are also used to illustrate the differences between the tests.

Simulations were carried out to generate 500,000 samples of the float range/baseline parameters and ambiguities for different models. The first step is to use a random generator to generate n independent samples from the univariate standard normal distribution $N(0, 1)$, and then collect these in a vector x. This vector is transformed by means of $\hat{a} = Gx$, with G equal to the Cholesky factor $Q_{\hat{a}} = GG^T$. The result is a sample $\hat{a}$ from $N(0, Q_{\hat{a}})$, and this sample is used as input for integer least-squares estimation. If the output of this estimator equals the null vector, then it is correct; otherwise it is incorrect. This process can be repeated N times, and one can count how many times the null vector is obtained as solution, say N_s times, and how often the outcome equals a nonzero integer vector, say N_f times. The approximations of the success rate and failure rate then follow as

$$P_s = N_s/N, \qquad P_f = N_f/N$$

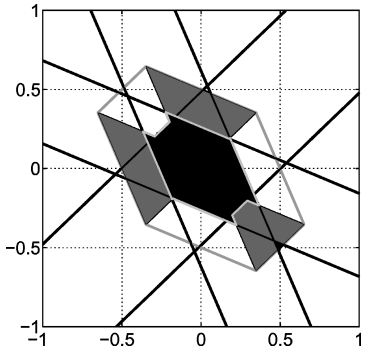

Fig. 4 Geometry of projector test aperture pull-in region (black) for Q_1, $\mu = 1$.

To get good approximations, the number of samples N must be chosen sufficiently large; see Ref. 22.

We will start with a two-dimensional example. The following variance matrices $Q_{\hat{a}}$ are used:

$$Q_1 = \begin{bmatrix} 0.0865 & -0.0364 \\ -0.0364 & 0.0847 \end{bmatrix}, \qquad Q_2 = Q_1 + \begin{bmatrix} 0.8 & 0 \\ 0 & 0 \end{bmatrix} \quad (39)$$

The first variance matrix corresponds to a dual-frequency GPS model for one satellite–receiver pair.

Figure 5 shows examples of the aperture pull-in regions for the different tests as obtained with two different failure rates. The aperture pull-in regions of the F-ratio test are not shown, because for the same failure rate the size of the corresponding regions still depends on the sample. Recall that the shape is identical to that of the ratio test aperture pull-in region.

The geometry of the regions obtained with the different discrimination tests was revealed in the previous sections, obviously resulting in quite different shapes. The shape of the optimal aperture pull-in region is determined by the probability distributions of the float ambiguities and the ambiguity residuals.

Especially with Q_1, the regions for the ratio test and optimal test are very similar. This is an explanation for why the performance of the ratio test is good in many practical situations. The regions are especially different in the direction of the vertices of the ILS pull-in region. That is because in those directions there are two second-best integer vectors such that $\|\hat{a} - \check{a}_2\|^2_{Q_{\hat{a}}} = \|\hat{a} - \check{a}_3\|^2_{Q_{\hat{a}}}$, but the squared norm on the right-hand side is not considered by the ratio test, whereas it does affect the size of the optimal test statistic. If the aperture parameter is chosen so that the optimal IA pull-in region just touches the ILS pull-in region, this results in the largest difference between the ratio test and optimal test. The reason is that for a large aperture parameter the optimal IA pull-in region is cut off by the ILS pull-in region. This is not the case for the ratio test pull-in region, because it starts to resemble the shape of the ILS pull-in region for large μ.

For Q_2, the difference between the tests seems to be much more significant. However, it should be noted that for this example there is a very low probability that $\hat{a}$ will fall into the region where the two aperture pull-in regions do not overlap, so that the performance of the two tests is still quite similar.

With respect to the difference test, conclusions similar to those for the ratio test can be drawn, although the difference from the optimal test is somewhat more significant. This is due to the shape of the aperture pull-in regions. Since these regions are bounded by planes, the pull-in regions are different not only from the optimal

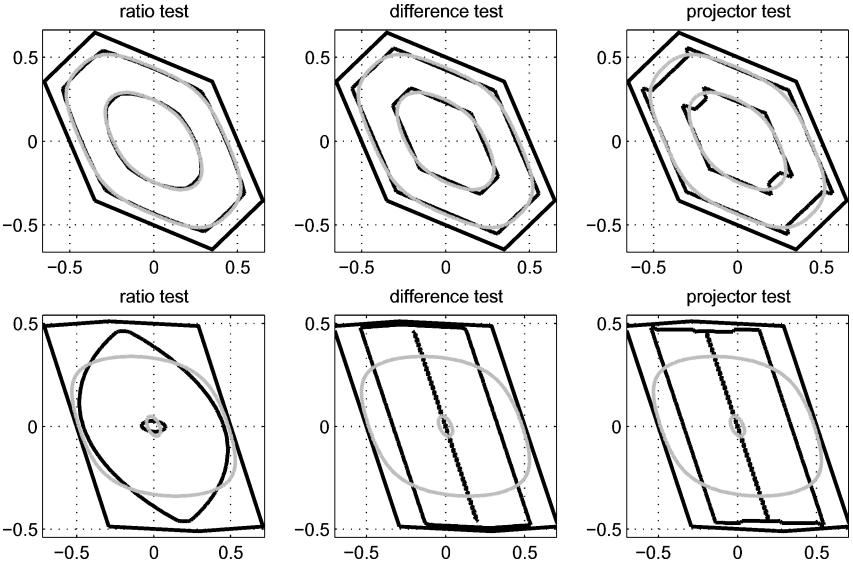

Fig. 5 Examples of two-dimensional aperture pull-in regions of the discrimination tests (black) and optimal test (gray) for two different failure rates. Top: Q_1, failure rates of 0.005 and 0.06; Bottom: Q_2, failure rates of 0.005 and 0.4.

IA pull-in regions in the direction of the vertices of the ILS pull-in region, but also in the direction of the adjacent integers.

The difference between the aperture pull-in regions of the optimal test and the projector test is much clearer than for the other two tests, due to the nonconvex shape of the region corresponding to the projector test.

To get an idea of the actual performance of the tests in practice, simulations are used for several geometry-based, dual-frequency GPS models. The GPS constellation is based on the Yuma almanac for GPS week 184 and a cut-off elevation of 15 deg. Undifferenced standard deviations of 30 cm and 3 mm are used for the code and phase observations, respectively. The GPS model is set up for a single epoch for two different times, at which four and six satellites were visible, respectively. The baseline length was chosen to be short to medium length by varying the ionospheric standard deviation σ_I. For the simulation 500,000 samples are used.

Table 1 shows the success rates as obtained with the various integer aperture estimators. Two different failure rates are used with each of the models. The results for Q_1, corresponding to a geometry-free model for two satellites, are also included. By definition the optimal integer aperture estimator will result in the highest success rates, but it turns out that the discrimination tests result in comparable success rates for most examples. The success rates obtained with the ratio test and the difference test are especially close to those obtained with optimal IA estimation.

Table 2 shows the percentage of decisions identical to the optimal test, based on a comparison of the decisions for each generated sample. This table confirms that indeed the ratio test and difference test perform close to optimally. The F-ratio test and the projector test clearly perform less close to optimally.

These results are as could be expected from the comparison of the aperture pull-in regions for the two-dimensional examples.

Table 1 Success rates obtained with our fixed failure rate approach for ratio test (R), F-ratio test (F-R), difference test (D), projector test (P), and optimal test (O)[a]

			Success rates				
No. SV	σ_I [cm]	P_f	R	F-R	D	P	O
2	0	0.005	0.369	0.318	0.365	0.363	0.369
		0.025	0.637	0.615	0.636	0.633	0.637
4	0	0.005	0.328	0.297	0.320	0.312	0.330
		0.025	0.550	0.536	0.543	0.532	0.552
4	1	0.005	0.026	0.021	0.025	0.025	0.026
		0.025	0.082	0.073	0.079	0.079	0.083
6	1	0.005	0.976	0.976	0.976	0.910	0.976
		0.010	0.987	0.987	0.987	0.978	0.987
6	3	0.005	0.025	0.023	0.027	0.027	0.031
		0.025	0.089	0.084	0.091	0.083	0.098

[a]The first two columns show the number of satellites (No. SV) and ionospheric standard deviation (σ_I) respectively.

Table 2 Percentage of decisions identical to optimal test for ratio test (R), F-ratio test (F-R), difference test (D), and projector test (P) if our fixed failure rate approach is used[a]

			% identical			
No. SV	σ_I [cm]	P_f	R	F-R	D	P
2	0	0.005	98.8	87.1	97.2	96.7
		0.025	99.2	92.6	97.6	96.5
4	0	0.005	97.8	91.0	95.6	93.9
		0.025	97.9	93.4	95.0	92.6
4	1	0.005	99.6	97.3	98.6	98.7
		0.025	98.6	93.7	96.0	96.1
6	1	0.005	99.6	99.6	99.9	92.0
		0.010	99.9	99.9	99.9	98.7
6	3	0.005	97.0	96.6	97.9	97.6
		0.025	93.8	92.7	94.9	92.7

[a]The first two columns show the number of satellites (No. SV) and ionospheric standard deviation (σ_I), respectively.

Table 3 Critical values obtained with our fixed failure rate approach for ratio test (R), F-ratio test (F-R), difference test (D), projector test (P), and optimal test (O)[a]

			Critical values				
No. SV	σ_I [cm]	P_f	R	F-R	D	P	O
2	0	0.005	0.106	0.160	7.803	0.888	1.031
		0.025	0.318	0.390	4.379	1.343	1.151
4	0	0.005	0.345	0.449	7.915	1.498	1.040
		0.025	0.551	0.640	4.837	1.848	1.167
4	1	0.005	0.187	0.343	5.670	0.772	1.253
		0.025	0.335	0.501	4.216	1.001	1.445
6	1	0.005	0.854	0.891	2.878	2.690	1.250
		0.010	0.977	0.983	0.440	3.499	1.844
6	3	0.005	0.392	0.609	6.095	0.476	1.206
		0.025	0.542	0.717	4.576	0.835	1.379

[a]The first two columns show the number of satellites (No. SV) and ionospheric standard deviation (σ_I), respectively.

Currently, in practice, the discrimination tests are used in combination with a fixed critical value. The results in Table 3 show that it is not desirable to do so, because it may result in tests that are either too conservative or too optimistic. From the table it follows that to obtain the same failure rate for differently models, the corresponding critical values must be chosen quite differently. For the ratio test a critical value of $\frac{1}{3}$ or 0.5 is often used.[2,53] The critical values obtained with the fixed failure rates in Table 3 are much larger or much smaller in most cases. Hence, the corresponding failure rates are either smaller or larger, depending on the model at hand. This is also true for the F-ratio test, for which a critical value of 0.5 is mostly used.[54] If the projector test statistic is assumed to have a (truncated) normal distribution, and the critical value is chosen based on a level of significance of 0.05, the corresponding failure rates vary between 0.000 for the model with six satellites and $\sigma_I = 1$ cm, and 0.487 for the model with four satellites and $\sigma_I = 1$ cm. The critical values of the difference test obtained for the model with six satellites and $\sigma_I = 1$ cm are very different from those obtained for the other models. Hence, the difference test applied with a fixed critical value will also result in different failure rates. Obviously, the approach of integer aperture estimation with a fixed failure rate is to be preferred above the traditional approaches.

Conclusions

In this contribution an overall approach is presented for the combined problem of integer estimation and validation. This approach, which is based on the theory of integer aperture estimation, for the first time includes an overall probabilistic evaluation of GNSS ambiguity resolution. With the freedom to set the size and shape of the aperture pull-in region, integer aperture estimation allows the user to get control over the failure rate of ambiguity resolution. It has been shown that the various integer discrimination tests that are in use in practice for integer validation are all members of the same class of integer aperture estimators. This common theoretical basis makes a rigorous comparison of their performances possible. By revealing the geometry of the aperture pull-in regions, further insight was gained into the driving mechanisms of the different discrimination tests.

We also presented the optimal integer aperture estimator. This is the estimator that maximizes the success rate for a user-given failure rate. It was given for an arbitrary PDF of the float solution. For the case of a multivariate normal distribution, the optimal estimator was compared to the discrimination tests, both in a qualitative and in a quantitative manner. In this comparison we identified some pitfalls and erroneous assumptions on which these tests were based in the literature. It also followed from the comparison that the ratio test and the difference test could both give a performance close to optimal. However, this performance is valid when our fixed failure rate approach is used, but not if the classical approach of using a fixed critical value is used.

The fixed-failure-rate approach implies that the aperture parameter, which governs the size of the pull-in region, is automatically

adapted to the strength of the underlying model. If the strength of the underlying model increases, for example, due to the use of more data or more precise data, the size of the aperture pull-in region will automatically increase, thus resulting in more frequent acceptance of the integer solution. Hence, with this approach the time to first fix will be shorter, while at the same time it is guaranteed that the probability of incorrect fixing is below a user-defined threshold.

References

[1]Hofmann-Wellenhof, B., Lichtenegger, H., and Collins, J., *Global Positioning System: Theory and Practice*, 5th ed., Springer-Verlag, Berlin, 2001.

[2]Leick, A., *GPS Satellite Surveying*, 3rd ed., Wiley, New York, 2003.

[3]Parkinson, B. W., and Spilker, J. J. (eds.), *Global Positioning System: Theory and Applications, Vols. 1 and 2*, Progress in Aeronautics and Astronautics, Vol. 164, AIAA, Washington, DC, 1996.

[4]Strang, G., and Borre, K., *Linear Algebra, Geodesy, and GPS*, Wellesley–Cambridge Press, Wellesley, MA, 1997.

[5]Teunissen, P. J. G., and Kleusberg, A., *GPS for Geodesy*, 2nd ed., Springer-Verlag, Berlin, 1998.

[6]Kim, U. S., De Lorenzo, D. S., Akos, D., Gautier, J., Enge, P., and Orr, J., "Precise Phase Calibration of a Controlled Reception Pattern GPS Antenna for JPALS," *Proceedings of IEEE PLANS'04*, Inst. of Electrical and Electronics Engineers, New York, 2004, pp. 478–485.

[7]De Lorenzo, D. S., Alban, S., Gautier, J., Enge, P., and Akos, D., "GPS Attitude Determination for a JPALS Testbed: Integer Initialization and Testing," *Proceedings of IEEE PLANS'04*, Inst. of Electrical and Electronics Engineers, New York, 2004, pp. 762–770.

[8]Crassidis, J. L., Markley, F. L., and Lightsey, E. G., "Global Positioning System Integer Ambiguity Resolution Without Attitude Knowledge," *Journal of Guidance, Control, and Dynamics*, Vol. 22, No. 2, 1999, pp. 212–218.

[9]Peng, H. M., Chang, F. R., and Wang, L. S., "Attitude Determination Using GPS Carrier Phase and Compass Data," *Proceedings of ION NTM-1999*, The Inst. of Navigation, Fairfax, VA, 1999, pp. 727–732.

[10]Bell, T., "Global Positioning System-Based Attitude Determination and the Orthogonal Procrustes Problem," *Journal of Guidance, Control, and Dynamics*, Vol. 26, No. 5, 2003, pp. 820–822.

[11]Park, C. S., and Teunissen, P. J. G., "A New Carrier Phase Ambiguity Estimation for GNSS Attitude Determination Systems," *Proceedings of International Symposium on GPS/GNSS*, Japan GPS Council, Tokyo, 2003, pp. 249–255.

[12]Leung, S., and Montenbruck, O., "Real-Time Navigation of Formation Flying Spacecraft Using GPS Measurements," *Journal of Guidance, Control, and Dynamics*, Vol. 28, No. 2, 2005, pp. 226–235.

[13]Kroes, R., Montenbruck, O., Bertiger, W., and Visser, P., "Precise GRACE Baseline Determination Using GPS," *GPS Solutions*, Vol. 9, No. 1, 2005, pp. 21–31.

[14]Betti, B., Crespi, M., and Sansò, F., "A Geometric Illustration of Ambiguity Resolution in GPS Theory and a Bayesian Approach," *Manuscripta Geodaetica*, Vol. 18, No. 6, 1993, pp. 317–330.

[15]Gundlich, B., "Statistische Untersuchung Ganzzahliger und Reellwertiger Unbekannter Parameter im GPS-Modell," Ph.D. Dissertations, DGK, Reihe C, No. 549, Munich, 2002.

[16]Gundlich, B., and Koch, K. R., "Confidence Regions for GPS Baselines by Bayesian Statistics," *Journal of Geodesy*, Vol. 76, No. 1, 2002, pp. 55–62.

[17]Gundlich, B., and Teunissen, P. J. G., "Multiple Models: Fixed, Switching and Interacting," *V. Hotine-Marussi Symposium on Mathematical Geodesy*, edited by F. Sansò, IAG Symposia, No. 127, Springer-Verlag, Berlin, 2004.

[18]De Lacy, M. C., Sansò, F., Rodriguez-Caderot, G., and Gil, A. J., "The Bayesian Approach Applied to GPS Ambiguity Resolution. A Mixture Model for the Discrete–Real Ambiguities Alternative," *Journal of Geodesy*, Vol. 76, No. 2, 2002, pp. 82–94.

[19]Teunissen, P. J. G., "Theory of Integer Equivariant Estimation with Application to GNSS," *Journal of Geodesy*, Vol. 77, No. 7–8, 2003, pp. 402–410.

[20]Teunissen, P. J. G., "Integer Aperture GNSS Ambiguity Resolution," *Artificial Satellites*, Vol. 38, No. 3, 2003, pp. 79–88.

[21]Jonkman, N. F., "Integer GPS Ambiguity Estimation Without the Receiver–Satellite Geometry," LGR Series, No. 18, Delft Geodetic Computing Centre, Delft Univ. of Technology, 1998.

[22]Teunissen, P. J. G., "On the Integer Normal Distribution of the GPS Ambiguities," *Artificial Satellites*, Vol. 33, No. 2, 1998, pp. 49–64.

[23]Teunissen, P. J. G., "An Optimality Property of the Integer Least-Squares Estimator," *Journal of Geodesy*, Vol. 73, No. 11, 1999, pp. 587–593.

[24]Teunissen, P. J. G., "The Parameter Distributions of the Integer GPS Model," *Journal of Geodesy*, Vol. 76, No. 1, 2002, pp. 41–48.

[25]Teunissen, P. J. G., "A Theorem on Maximizing the Probability of Correct Integer Estimation," *Artificial Satellites*, Vol. 34, No. 1, 1999, pp. 3–9.

[26]Teunissen, P. J. G., "Least Squares Estimation of the Integer GPS Ambiguities," Invited lecture, Section IV, *Theory and Methodology, IAG General Meeting*, International Association of Geodesy, Budapest, 1993.

[27]Teunissen, P. J. G., "The Least-Squares Ambiguity Decorrelation Adjustment: A Method for Fast GPS Integer Ambiguity Estimation," *Journal of Geodesy*, Vol. 70, No. 1–2, 1995, pp. 65–82.

[28]De Jonge, P. J., and Tiberius, C. C. J. M., "The LAMBDA Method for Integer Ambiguity Estimation: Implementation Aspects," LGR Series, No. 12, Delft Geodetic Computing Centre, Delft Univ. of Technology, 1996.

[29]Boon, F., and Ambrosius, B., "Results of Real-Time Applications of the LAMBDA Method in GPS-Based Aircraft Landings," *Proceedings of the International Symposium on Kinematic Systems in Geodesy, Geomatics and Navigation*, Dept. of Geomatics Engineering, Univ. of Calgary, Calgary, Canada, 1997, pp. 339–345.

[30]Boon, F., De Jonge, P. J., and Tiberius, C. C. J. M., "Precise Aircraft Positioning by Fast Ambiguity Resolution Using Improved Troposphere Modelling," *Proceedings of ION GPS-1997*, The Inst. of Navigation, Fairfax, VA, 1997, pp. 1877–1884.

[31]Chaitin-Chatelin, F., Dallakyan, and Frayssé, V., "On the GPS Carrier Phase Ambiguity Resolution. The LAMBDA Method: An Analysis of Speed, Efficiency and Numerical Robustness," TR IR/PA/99/23, Cerfacs, 1999.

[32]Cox, D. B., and Brading, J. D. W., "Integration of LAMBDA Ambiguity Resolution with Kalman Filter for Relative Navigation of Spacecraft," *Navigation*, Vol. 47, No. 3, 2000, pp. 205–210.

[33]De Jonge, P. J., and Tiberius, C. C. J. M., "Integer Ambiguity Estimation with the LAMBDA Method," *IAG Symposia No. 115, GPS Trends in Terrestrial, Airborne and Spaceborne Applications*, edited by G. Beutler, Springer-Verlag, New York, 1996, pp. 280–284.

[34]Han, S., "Ambiguity Resolution Techniques Using Integer Least-Squares Estimation for Rapid Static or Kinematic Positioning," *Proceedings of Symposium Satellite Navigation Technology and Beyond*, Paper 34, Space Centre for Satellite Navigation, Queensland Univ. of Technology, Brisbane, Australia, 1995, p. 10.

[35]Kiamehr, R., "Comparison of Ambiguity Resolution Using LAMBDA and KTH Method," *Proceedings of 2003 International Symposium on GPS/GNSS*, Japan GPS Council, Tokyo, 2003.

[36]Lee, H. K., Wang, J., and Rizos, C., "An Integer Ambiguity Resolution Procedure for GPS/Pseudolite/INS Integration," *Journal of Geodesy*, Vol. 79, No. 4–5, 2005, pp. 242–255.

[37]Milbert, D., "Influence of Pseudorange Accuracy on Phase Ambiguity Resolution in Various GPS Modernization Scenarios," *Navigation*, Vol. 52, No. 1, 2005, pp. 29–38.

[38]Tiberius, C. C. J. M., and De Jonge, P. J., "Fast Positioning Using the LAMBDA Method," *Proceedings of DSNS'95*, Paper 30, The Nordic Inst. of Navigation, Oslo, 1995.

[39]Tiberius, C. C. J. M., Teunissen, P. J. G., and De Jonge, P. J., "Kinematic GPS: Performance and Quality Control," *Proceedings of KIS'97*, Dept. of Geomatics Engineering Univ. of Calgary, Calgary, Canada, 1997, pp. 289–299.

[40]Weiming, T., "Ambiguity Resolution of Single Epoch Single Frequency Data with Baseline Length Constraints Using LAMBDA Method," *Proceedings of 2004 International Symposium on GPS/GNSS*, Univ. of New South Wales, Sydney, Australia, 2004.

[41]Zhou, Y., and Liu, J., "Another Form for LAMBDA Method," *Geospatial Information Science*, Vol. 6, No. 3, 2003, pp. 66–70.

[42]De Jonge, P. J., Tiberius, C. C. J. M., and Teunissen, P. J. G., "Computational Aspects of the LAMBDA Method for GPS Ambiguity Resolution," *Proceedings of ION GPS-1996*, The Inst. of Navigation, Fairfax, VA, 1996, pp. 935–944.

[43]Xu, P., "Random simulation and GPS Decorrelation," *Journal of Geodesy*, Vol. 75, No. 7, 2001, pp. 408–423.

[44]Svendsen, J. G. G., "Some Properties of Decorrelation Techniques in the Ambiguity Space," *GPS Solutions*, [online Journal], Vol. 10, No. 1, 2006, pp. 40–44, DOI: 10.1007/s10291-005-0004-6, 2005.

[45]Lou, L., and Grafarend, E., "GPS Integer Ambiguity Resolution by Various Decorrelation Methods," *Zeitschrift für Vermessungswesen*, Vol. 128, No. 3, 2003, pp. 203–210.

[46]Chang, X. W., Yang, X., and Zhou, T., "A Modified LAMBDA Method for Integer Least-Squares Estimation," *Journal of Geodesy*, Vol. 79, No. 9, 2005, pp. 552–565.

[47]Verhagen, S., "On the Reliability of Integer Ambiguity Resolution," *Navigation*, Vol. 52, No. 2, 2005, pp. 99–110.

[48]Abidin, H. A., "Computational and Geometrical Aspects of On-the-Fly Ambiguity Resolution," Ph.D. Dissertation, TR 104, Univ. of New Brunswick, 1993.

[49]Chen, Y., "An Approach to Validate the Resolved Ambiguities in GPS Rapid Positioning," *Proceedings of the International Symposium on Kinematic Systems in Geodesy, Geomatics and Navigation*, Dept. of Geomatics Engineering, Univ. of Calgary, Calgary, Canada, 1997, pp. 301–304.

[50]Euler, H. J., and Schaffrin, B., "On a Measure for the Discernibility Between Different Ambiguity Solutions in the Static–Kinematic GPS-Mode," IAG Symposia No. 107, *Kinematic Systems in Geodesy, Surveying, and Remote Sensing*, Springer-Verlag, New York, 1991, pp. 285–295.

[51]Frei, E., and Beutler, G., "Rapid Static Positioning Based on the Fast Ambiguity Resolution Approach FARA: Theory and First Results," *Manuscripta Geodaetica*, Vol. 15, No. 6, 1990, pp. 325–356.

[52]Han, S., "Quality Control Issues Relating to Instantaneous Ambiguity Resolution for Real-Time GPS Kinematic Positioning," *Journal of Geodesy*, Vol. 71, No. 6, 1997, pp. 351–361.

[53]Han, S., and Rizos, C., "Validation and Rejection Criteria for Integer Least-Squares Estimation," *Survey Review*, Vol. 33, No. 260, 1996, pp. 375–382.

[54]Landau, H., and Euler, H. J., "On-the-Fly Ambiguity Resolution for Precise Differential Positioning," *Proceedings of ION GPS-1992*, The Inst. of Navigation, Fairfax, VA, 1992, pp. 607–613.

[55]Wang, J., Stewart, M. P., and Tsakiri, M., "A Discrimination Test Procedure for Ambiguity Resolution On-the-Fly," *Journal of Geodesy*, Vol. 72, No. 11, 1998, pp. 644–653.

[56]Verhagen, S., "Integer Ambiguity Validation: An Open Problem?" *GPS Solutions*, Vol. 8, No. 1, 2004, pp. 36–43.

[57]Verhagen, S., and Teunissen, P. J. G., "On the Probability Density Function of the GNSS Ambiguity Residuals," *GPS Solutions* [online journal], Vol. 10, No. 1, 2006, pp. 21–28, DOI: 10.1007/s10291-005-0148-4, 2005.

[58]Teunissen, P. J. G., "GNSS Ambiguity Resolution with Optimally Controlled Failure-Rate," *Artificial Satellites*, Vol. 40, No. 4, 2005, pp. 219–227.

[59]Teunissen, P. J. G., "Penalized GNSS Ambiguity Resolution," *Journal of Geodesy*, Vol. 78, No. 4–5, 2004, pp. 235–244.

[60]Teunissen, P. J. G., and Verhagen, S., "On the Foundation of the Popular Ratio Test for GNSS Ambiguity Resolution," *Proceedings of ION GNSS-2004*, The Inst. of Navigation, Fairfax, VA, 2004, pp. 2529–2540.

[61]Teunissen, P. J. G., "GPS Carrier Phase Ambiguity Fixing Concepts," *GPS for Geodesy*, edited by P. J. G. Teunissen and A. Kleusberg, Springer-Verlag, Berlin, 1998, Chap. 8.